

Visual marker based shape recognition system for continuum manipulators ^{*}

Jan Fraś, Sebastain Tabaka, and Jan Czarnowski

Przemysłowy Instytut Automatyki i Pomiarów, PIAP
al.Jerozolimskie 202, 02-486 Warsaw, Poland
{jfras,stabaka}@piap.pl
czarnowski.jan@gmail.com

Abstract. Soft robotics is young and popular research area. Continuum robots do not have traditional joints and their movement is generated by smooth deformation of their body. They are made of flexible materials which results in very complex shapes they can take. Due to complex kinematics and soft materials they are composed of, soft manipulator sensing is very demanding issue. Despite a number of custom sensors that have been proposed, data gathered by them is not sufficient for effective shape reconstruction. In this paper authors propose a system that enables efficient shape reconstruction for soft pneumatic manipulator. System is based on custom physical model and vision system composed of video camera and two-dimensional optical markers.

1 Introduction

Soft continuum robotics is a young robotics research area. It focuses on design and control of flexible manipulators that have no traditional prismatic or rotational joints. Such manipulators are manufactured using innovative soft materials that are safe in contact with external objects and enables the robot to achieve shapes that are unreachable for conventional manipulators. These properties make soft manipulators very promising from challenging tasks point of view especially for minimal invasive surgery or soft objects manipulation [1], [2]. From the control point of view the main difference between soft and conventional robotics is their continuum kinematics. Continuum manipulator movement is generated by smooth deformation of its body. Since there are no rigid parts connected by well defined joints, the shape reconstruction is not trivial and thus, control of the manipulator shape is difficult as well. Soft manipulators can be driven by tendons or fluids, but in both cases actuation results not only in rotation or translation of some manipulator part, but much more complex deformation of the manipulator structure. In traditional case manipulator any deformation is immediately recorded by encoders housed in joints and due to that can be easily encompassed. What makes the shape detection task really complex is that

^{*} Part of the work described in this paper is funded by the Seventh Framework Programme of the European Commission in the framework of EU project STIFF-FLOP

every external force applied to the manipulator causes it to deform and the deformation is distributed along it, so it can not be easily compensated. Moreover there are no reliable sensors available for proper shape detection. In traditional robotics sufficient sensors are for example rotational encoders, but that is no such case. Many sensors were proposed but since soft robot can deform to very complex shapes the data they provide individually is not satisfying for effective manipulator control [3], [4], [5].

In this paper we present a specific soft manipulator design, custom physical model of it and an external single-camera positioning system that coupled with the model provides a complete robot shape reconstruction. Due to low hardware requirements (single camera) the system can be applied to minimal invasive surgery.

2 Manipulator design

The manipulator used in the experiment is composed of two identical modules, three degrees of freedom each (figure 1). The module is able to bend in any direction and elongate.

Single module consists of three symmetrically deployed pneumatic actuators and an empty central channel for pressure pipes and possible actuator or sensors cables. Module body is made of EcoFlex 0050 silicone and manufactured by molding in steps. Each actuation chamber is composed of two symmetrical cylinders reinforced by single nylon thread applied in a tight helix around each cylinder (figure 1). Such reinforcement limits radial cylinder expansion when pressurized and allows its elongation in the same time. Pressurization of a single actuation chamber causes it to elongate, which results in module bending. Cylindrical shape was chosen for the actuator because spherical cross-section is the only shape that does not change its geometry while internal pressure applied. Cylinders are coupled in order to gain the activation capabilities by increasing the chamber cross-section area. For more information see [6].



Fig. 1: Single module design. On the left: module; on the right: module cross-section, reinforced actuation chambers and central channel visible

3 Manipulator modeling

In order to determine the shape of the manipulator, a proper model had to be designed and implemented. Since the manipulator arm is designed to operate in tight spaces, there is high probability of contact with other bodies. This fact makes calculating the influence of external forces acting on the arm a must. This significant factor is not considered by the popular Constant Curvature model of continuous robots [7], [8], what renders it unusable in this case. For the model described in this paper, following assumptions had been made: the segment is made of homogeneous material of known stiffness, with three pressure chambers hollowed out; the dimensions of cross-section of the pressure chambers are constant (provided by the braiding); the pressure in chambers is constant at any point. The other influence of the braiding has been neglected. Since the arm consists of two separately actuated segments (modules), equations for a single segment are presented.

The segment is controlled by changing the pressure in the chambers. Forces resulting from the inner pressure are parallel with module Z-axis (perpendicular to the cross section) in each cross-section. Therefore the resulting moment causes pure bending of the module. Because the chamber diameter and pressure is constant throughout the whole module length, the resulting bending moment is also constant. Elongation at any point along the module's axis can be described using the Hooke's Law. The force causing module stretching is calculated by adding forces resulting from each chamber pressure.

The external forces influence has to also be represented in bending, torsion and elongation calculation. For simplification the external force is assumed to act on the module tip. External force causes additional moment to appear in all module's cross sections. The force and moment at specific cross section depend on its position. Knowing the relative orientation of tip frame in the frame of the cross section and combining it with the force and moment resulting from pressures, one can calculate the overall force and moment acting on that cross section. Those values can be then used to determine the elongation and curvature of the module at point P. Shape of the module can be determined by integrating the elongation, twist and bend of every point along the module axis. For more information see [5].

4 External absolute positioning system

There are commercial systems available for absolute pose measurement. Depending on the desired application systems have different properties and provide different kinds of data. One of the systems is the Aurora Electromagnetic Tracing System [9] that provides sub-millimetric and sub-degree tracking for a specific marker provided with the system. The main problem with the system is that it generates the electro-magnetic field in order to measure the marker pose and thus is very sensitive to presence of metallic objects in the measurement area, which makes it useless in many cases. Other option is to measure the manipulator shape using the surface detecting systems such as Microsoft Kinect [10].

In this case the measurement device has significant dimensions and can not be applied to many scenarios as well (for example minimal invasive surgery). Due to the limitations of the current systems the proposed solution is based on ordinary vision camera and visual two dimensional markers. Size is not an issue for present cameras, and even very small camera provides high image quality. Moreover optical camera does not affect the measured area in any way (no physical contact or any field generation). Moreover cameras are already present in medical operational field, so medical application of such solution would not require any additional equipment or certification.

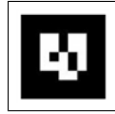


Fig. 2: An example of two-dimensional marker.

The system is based on two-dimensional graphical markers. These markers are built from white and black squares, which can be grouped to form larger monochrome areas in which marker's identification number (ID) is coded (figure 2). To calculate the marker's position and orientation and detect its ID the Chilitags [11] computer programming library is used.

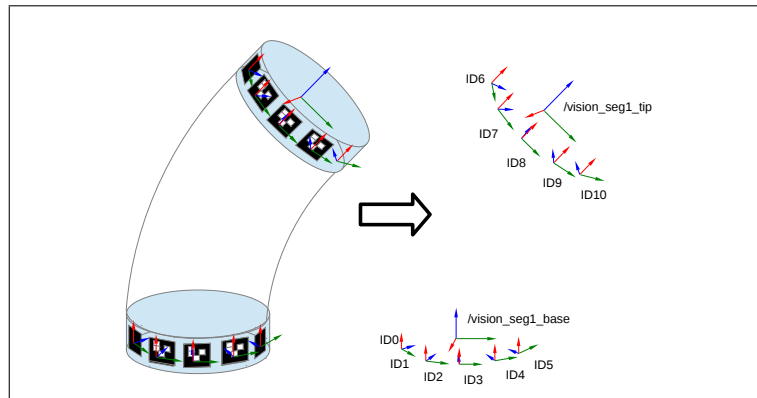


Fig. 3: Vision system principle

The system is equipped with video camera (GigE, 1936 x 1458, 30 fps) and camera lens (manual focus, focal length 6 mm). Markers are attached around each segment's base and a tip on rings (figure 3). First segment's tip is connected to the second segment's base.

The marker detection library detects 2D markers on the image acquired from

the camera and calculates their position and orientation in a camera's coordinate frame. Both camera's and markers' position were measured and are well-known. Having all these data and transformations it is possible to obtain the soft-manipulator's global position and orientation. Translation and rotation of a single marker is always connected with the soft-manipulator's displacement.

4.1 Marker detection precision

With a static lighting conditions and correct camera calibration, the quality of single marker detection depends mainly on a marker's size, distance from the camera and its orientation. Bad marker detection results in incorrect soft-manipulator's final position calculation.

Markers on the soft-manipulator are placed on a ring, so the camera does not see all of them at the same angle. Observations of the soft-manipulator shape recognition system behavior showed that marker which was perpendicular to the camera's optical axis gave more unstable position due to the problems with a right marker's perspective detection. Therefore, small detection errors on the image plane had a great effect on the marker's rotation. Sometimes there were also problems with markers which were under the high angle to the camera optical axis.

Marker detection validation To select the best marker's size for the soft-manipulator which would be detected without much noise caused by a distance from the camera and marker orientation research was made. Three sizes of a marker were checked: 0.5 cm, 1 cm and 2 cm. Using larger markers makes no sense, because they would be too large for the manipulator. Each marker has also been checked on a three different distances from the camera: 15 cm, 30 cm and 45 cm. The camera was always in a static position, only markers were moved and rotated around its vertical axis.

For each setup 50 samples were gathered and analyzed. Data analysis was based on calculating the average of detected marker's orientation (eq. 1) and their standard deviation (eq. 2).

$$\mu = \frac{1}{N} \sum_{i=1}^N x_i \quad (1)$$

$$S_n = \sqrt{\frac{1}{N} \sum_{i=1}^N (x_i - \mu)^2} \quad (2)$$

After changing distance of the markers to the camera, there was a need to refocus camera to get the most possible sharp marker's edges. After this operation camera stayed calibrated during the rest of the experiments.

According to the experiment, the smallest marker (0.5 cm) gives good results only for the shortest distance from the camera (15 cm). However, if an angle is lower than 20 degrees, detection problems occur (figure 5). Marker sometimes is

detected with a flipped orientation (figure 4) and its position is very noisy. For a 30 cm distance from the camera marker was nearly unrecognizable. It was only detected when the angle was lower than 60 degrees, but detection quality was very poor (figure 5). For a further distance (45 cm) marker was completely not detected.

Larger marker's size (1 cm) gives much better results for a distance from the camera equals 15 cm (figure 6). Marker was perfectly detected even when the angle was high. Unfortunately, that marker's size was not enough for further distances from the camera (30 cm and 45 cm) (figure 6). There was a lot of noise in a detected marker's orientation. Best results were achieved for a marker's size 2 cm. For an every distance detection quality was very satisfying (figure 7).

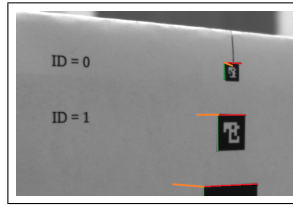


Fig. 4: The smallest marker's orange axis (Z) is flipped over in a wrong direction due to detection problems.

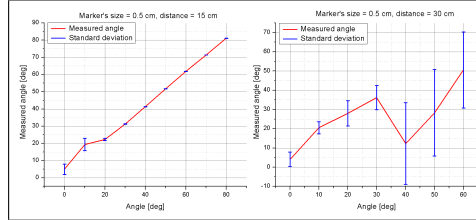


Fig. 5: Marker's size 0.5 cm detection quality.

5 Soft robotics system setup

As explained in the introduction, the shape reconstruction quality has great impact on the manipulator controlling possibilities. In this paper we propose an efficient system that provides complete shape reconstruction for the manipulator controlling task. System overview is presented in figure 8.

The system consist of a pressure supply, vision marker detection component and shape reconstruction software. Pressure supply provides actuation chambers with pressure and gives pressure measurement for shape reconstruction.

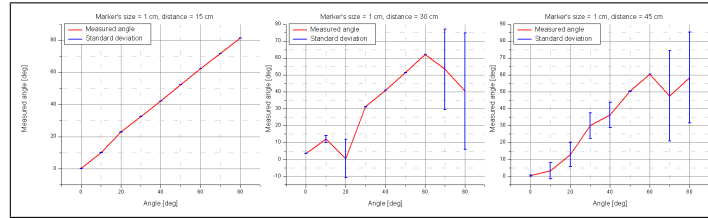


Fig. 6: Marker's size 1 cm detection quality.

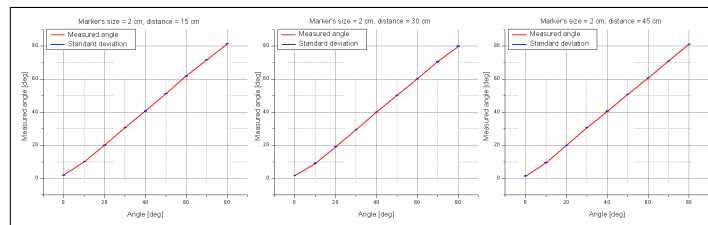


Fig. 7: Marker's size 2 cm detection quality.

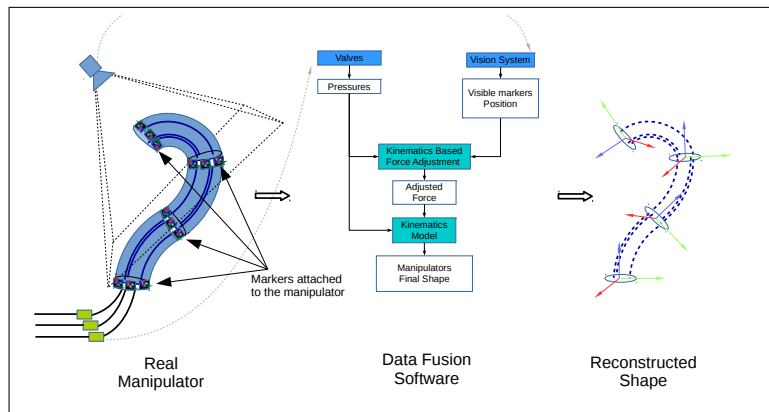


Fig. 8: Shape recognition system overview

The shape reconstruction block requires the pressures and forces acting on the manipulator. Pressure values are measured and provided directly by the valves powering the actuators, but force measurement is not easy task. Some custom sensors for soft robotics has been proposed, but all of them suffers form issues that makes them useless in real use cases. Some of them are able to measure force with good precision, but are able to measure the force only in finite number of discrete points. Therefore any force applied in between the sensors can not be measured and its effect on the manipulator is unnoticed by the model. Other solution are sensors that are capable to measure torque. There are commercial devices available, but the manipulator construction requires circular sensor shape and some room in the sensor axis for wires. There was a custom promising sensor proposed [4], but it is still in the development stage, and current performance is not sufficient for reliable shape reconstruction. Due to those issues a counterfactual solution has been proposed. The solution is based on the kinematics described above and the absolute pose measurement provided by the vision system. The measured pressure values (that are assumed to be of good quality) are supplied to the model, that produces the initial shape approximation. Error of the calculated poses of predefined points along the manipulator that markers are attached to can be calculated in relation to the measurement. Then the position error gradient is obtained in the external disturbances space. The disturbance space can be arbitrary defined. The simplest option is to assume that a three-dimensional force can act in any of the defined points. Using the gradient descent algorithm the forces that minimize the position error are obtained. The forces and the pressures are then supplied to the kinematics algorithm and the overall shape is calculated.

The solution provides force approximation that guarantee proper manipulator shape reconstruction for some range of forces. The reconstructed shape minimizes error of the position of known points and provides smooth approximation in between those points.

5.1 Experimental setup

The proposed algorithm has been tested in three test cases. In the first case only pressure has been applied to the lower manipulator segment. In second one the force only was acting on the manipulator. The force was applied to the upper part of the tip module. At the last case the pressure and the force was acting on the manipulator simultaneously. All the cases are presented in figures 9 to 11. In the first case the real manipulator is bended significantly more than it would result from internal pressures. Since manipulator is made of silicone the the gravity is able to generate an bending as shown. The algorithm successfully approximates the gravitation force, and resulting shape is similar to the real manipulator configuration. In the second case no pressure is provided. Thus the simulation expects its body to be straight. The forces deduced from vision system bends the simulated manipulator in similar way the real ones as well. Simulation without forces is presented in green, yellow color represents the simulated manipulator shape with forces taken into account. The aproximated forces are represented by

red arrows. The algorithm was launched for two possible points that simulated forces could act on: tip of the first and the tip of the second module.

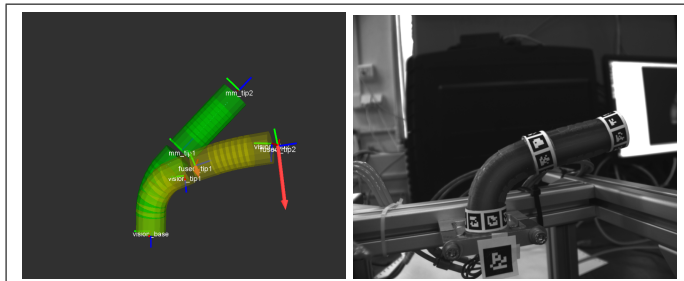


Fig. 9: Actuated lower module, no external force acting on the manipulator. Gravity influence visible.

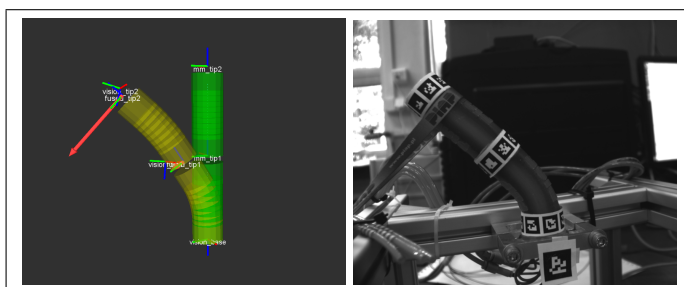


Fig. 10: No pressure supplied to the manipulator. External force acting on the upper module.

6 Conclusion and future work

Since the force values are only approximated and the number of points those position are measured is finite, the accuracy of the reconstructed shape is not in 100% correct. The force can be applied in any point on the manipulator surface, but algorithm assumes that there are only a few such points. There are other assumptions made that simplifies the real module, and those are the error source too. Moreover the marker reconstruction is not perfect so even if the model was perfect, the position of points that it would fit to are not perfectly measured too.

The proposed system potential usability has been shown, but additional work

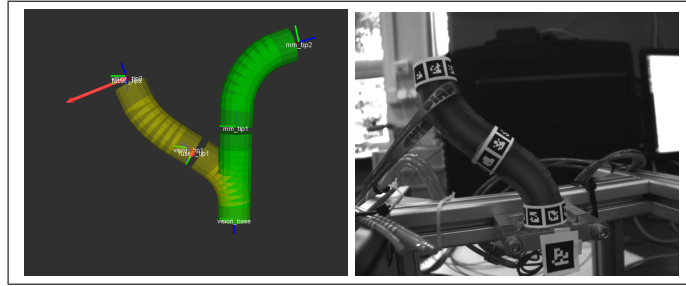


Fig. 11: Upper module actuated. Force acting on the upper module.

is required. In the future authors plan to perform quantitative tests with support of some commercial absolute measurement system (Aurora, Kinect, etc) to describe the algorithm operational space. Different marker position and number configuration will be tested.

References

1. Amir Degani, Howie Choset, Alon Wolf, Marco Zenati, "Highly articulated robotic probe for minimally invasive surgery", International Conference on Robotics and Automation, 2006
2. Cianchetti M, Ranzani T, Gerboni G, Nanayakkara T, Althoefer K, Dasgupta P, Menciassi A (2014) "Soft robotics technologies to address shortcomings in today's minimally invasive surgery: the STIFF-FLOP approach" *Soft Robotics*, 1(2) 122-131
3. Thomas C. Searle, Kaspar Althoefer, Lakmal Seneviratne and Hongbin Liu, "An Optical Curvature Sensor for Flexible Manipulators", International Conference on Robotics and Automation, 2013
4. Y. Noh, S. Sareh, J. Back, H. Wurdemann, T. Ranzani, E. Secco, A. Faragasso, H. Liu, and K. Althoefer, "A three-axial body force sensor for flexible manipulators," IEEE International Conference on Robotics and Automation, 2014.
5. Fraś J., Czarnowski J., Macias M. and Głowka J., "Static Modeling of Multisection Soft Continuum Manipulator for Stiff-Flop project", Springer, 2014.
6. J. Fraś, J. Czarnowski, M. Macias, J. Głowka, M. Cianchetti, A. Menciassi, "New STIFF-FLOP module construction idea for improved actuation and sensing" IEEE International Conference on Robotics and Automation, 2015 Seattle
7. R. J. Webster and B. A. Jones, "Design and Kinematic Modeling of Constant Curvature Continuum Robots: A Review," *The International Journal of Robotics Research*, vol. 29, pp. 1661–1683, Nov. 2010
8. Matthias Rolf and Jochen J. Steil, "Constant curvature continuum kinematics as fast approximate model for the Bionic Handling Assistant", IEEE/RSJ International Conference on Intelligent Robots and Systems, 2012
9. Aurora, <http://www.ndigital.com/medical/products/aurora/>
10. Microsoft Kinect, <https://dev.windows.com/en-us/kinect>
11. ÉCOLE POLYTECHNIQUE FÉDÉRALE DE LAUSANNE
<http://chili.epfl.ch/softwarei>